Evaluating the anti-fibrotic potency of galunisertib in a human *ex vivo* model of liver fibrosis

Theerut Luangmonkong, Su Suriguga, Emilia Bigaeva, Miriam Boersema, Dorenda Oosterhuis, Koert P. de Jong, Detlef Schuppan, Henricus A.M. Mutsaers, Peter Olinga

Abstract

Liver fibrosis is a major cause of liver-related mortality. Yet, to date, no effective anti-fibrotic drug is available. Galunisertib, a TGF-β receptor type I kinase inhibitor, is a potential candidate for the treatment of liver fibrosis. Here, we evaluated the potency of galunisertib in a human *ex vivo* model of liver fibrosis. Anti-fibrotic potency and associated mechanisms were studied *ex vivo*, using both healthy and cirrhotic human precision-cut liver slices. Fibrosis related parameters, both transcriptional and translational level, were assessed after treatment with galunisertib. Galunisertib showed a prominent anti-fibrotic potency. Phosphorylation of SMAD2 was inhibited, while that of SMAD1 remained unchanged. In healthy and cirrhotic human livers, spontaneous transcription of numerous gene-encoding collagens including pro-collagen 1α1, collagen maturation, non-collagenous extracellular matrix (ECM) components, ECM remodeling, and selected ECM receptors, was significantly decreased. The reduction of fibrosis related transcription was paralleled by a significant inhibition of pro-collagen I C-peptide released by both healthy and cirrhotic human liver slices. Moreover, galunisertib showed similar anti-fibrotic potency in humans and rats. Galunisertib is an attractive drug to be further investigated for the treatment of liver fibrosis. Inhibition of SMAD2 phosphorylation is probably a central mechanism of action. In addition, blocking the production and maturation of collagens, as well as promoting their degradation are related to the anti-fibrotic action of galunisertib.

Introduction

Advanced liver fibrosis, and its end-stage condition cirrhosis, is characterized by aberrant and excessive accumulation of extracellular matrix (ECM) components, with architectural and vascular distortion, and an excessive risk for mortality due to functional liver failure, variceal bleeding, infection and emerging liver cancer [4-6]. Liver fibrosis is mainly caused by viral infections, chronic alcohol abuse, non-alcoholic steatohepatitis, and biliary/autoimmune diseases [6]. To date, liver transplantation remains the sole therapeutic option for advanced cirrhosis. Yet, transplantation is an invasive and high-risk surgical procedure, and limited to only few patients at need [7]. Thus, there is an urgent and unmet need for effective anti-fibrotic drugs.

Among the spectrum of mediators possessing profibrotic properties, transforming growth factor-beta 1 (TGF-β1) has always been recognized as a key profibrogenic cytokine in liver fibrosis [8-10]. TGF-β1 affects various liver-specific cells, including fibrogenic stimulation of hepatic stellate cells (HSCs) and portal fibroblasts towards excessive ECM producing myofibroblasts, the major effector cells of fibrosis [10-12]. In hepatocytes, TGF-β1 can induce apoptosis or mitogenic pathways leading to various pathological conditions [10, 13]. It is well established that TGF-β1 signaling in liver fibrosis is mediated by the transcription factor SMAD2 via activin receptor-like kinase (ALK) 5 [9, 10, 14]. Recently, it was discovered that TGF-β1 might also activate transcription factor SMAD1 via ALK1 signaling in certain cell types; however, the role of this pathway in liver fibrosis remains unclear [15, 16].

Even though inhibition of TGF-β1 signaling has been studied as a potential therapeutic target for fibrosis in the past [8, 9], there is currently no specific inhibitor in clinical studies for fibrosis. However, galunisertib, a TGF-β receptor type I kinase inhibitor, is presently studied for the treatment of different cancers, including hepatocellular carcinoma [8, 17-20]. Due to its mode of action and attractive pharmacokinetic/pharmacodynamic properties [17], galunisertib may also qualify as a potential candidate for the treatment of liver fibrosis.

Previously, rodent and human *ex vivo* model of liver fibrosis, precision-cut liver slices (PCLS), have been successfully used to test the potency of a variety of putative anti-fibrotic compounds [21-23]. The main advantages of PCLS pertain to the fact that all cell types are preserved in their original environment and the possibility for studying in human tissues. Therefore, our study aimed to evaluate the anti-fibrotic potency of galunisertib in both early-onset and end-stage of fibrosis in human PCLS, as an immediate translation towards further studies. The use of human PCLS therefore permitted to study potency and possibly divergent molecular mechanism of action of galunisertib between rodents and human livers.

Chapter 4

Results

Spontaneous fibrosis in cultured PCLS
ATP content of the PCLS increased at the start of culture and remained constant for 48h (hPCLS and chPCLS) and 72h (rPCLS) (Figure 1A-C) indicating that the viability of the PCLS was maintained during culture.

Quantitative PCR revealed that, at the start of culture (0h), the basal expression of *COL1A1*, *α-SMA* and *PAI-1* in hPCLS and chPCLS was significantly higher than those of rPCLS. Furthermore, the expression of *COL1A1* and *TGF-β1* was significantly higher in chPCLS as compared to hPCLS (Supporting Information Figure S1).

Nonetheless, we observed a spontaneous onset of fibrogenesis during culture, as revealed by an increase in a multitude of fibrosis markers. In rPCLS, *Pai-1* levels were markedly elevated at 24h up till 72h. At the latter time point, gene expression of *Col1a1*, *Hsp47* and *α-Sma* was also significantly increased (Figure 1D). In hPCLS, *TGF-β1* levels increased at 24h up till 48h, at which time *COL1A1* and *FN2* expression was also upregulated (Figure 1E). In contrast, none of the fibrosis markers were modulated in chPCLS (Figure 1F).

On a protein level, expression of HSP47 and α-SMA was markedly increased up to 48h in both hPCLS and chPCLS (Figure 1H-I). Moreover, TGF-β1 signaling was active in these PCLS, as illustrated by the presence of phosphorylated SMAD1 and SMAD2. Conversely, no changes were observed in rPCLS (Figure 1G). Taken together, it is clear that fibrosis can be induced in different types of PCLS by culture activation.

Effect of galunisertib on spontaneous fibrosis
The impact of galunisertib on the fibrotic response in cultured PCLS was subsequently investigated. None of the tested concentrations of galunisertib affected PCLS viability (Figure 2).

In rPCLS, galunisertib appeared to concentration-dependently inhibit gene expressions of *Col1a1*, *Hsp47*, and *α-Sma*, up to 92%, 50%, and 83%, respectively, whereas *Pai-1*, *Fn2*, and *Tgf-β1* levels remained unchanged. However, statistically significant differences were found at the highest tested concentration (10 μM; Figure 3A). In hPCLS, *COL1A1* and *TGF-β1* gene expression were concentration-dependently inhibited, up to 78% and 40%, respectively (Figure 3B). Moreover, galunisertib significantly inhibited *COL1A1* (81%), *HSP47* (34%), *PAI-1* (54%), and *TGF-β1* (47%), gene expression in chPCLS (Figure 3C).

Effect of galunisertib on TGF-β1-induced fibrosis
Next, we studied whether the anti-fibrotic effect of galunisertib could also be observed in the presence of exogenous TGF-β1. Exposure to TGF-β1 significantly upregulated the expression of *Col1α1*, *Hsp47*, and *α-Sma*, at least 2-fold in rPCLS, and these upregulations were

significantly mitigated by galunisertib treatment (Figure 4A). Conversely, TGF-β1 did not increase the expression of the fibrosis markers in hPCLS (Figure 4B) and chPCLS (Figure 4C). Nonetheless, in the presence TGF-β1, galunisertib still reduced the gene expression of *COL1A1*, *HSP47*, *α-SMA* and *TGF-β1* in both hPCLS and chPCLS (Figure 4B-C).

Furthermore, Western blotting revealed that treatment with TGF-β1 upregulated Hsp47 and α-Sma protein expression in rPCLS, which was significantly antagonized by galunisertib (Figure 5A). This anti-fibrotic effect was not generally observed in hPCLS (Figure 5B) and chPCLS (Figure 5C); however, the effect of TGF-β1 and galunisertib in human PCLS was extremely variable (Supporting Information Figure S2).

Activation of TGF-β1 signaling in rPCLS by TGF-β1 was illustrated by a marked increase of SMAD2 phosphorylation (Figure 5A). Again, this downstream activation was not clearly seen in hPCLS (Figure 5B) and chPCLS (Figure 5C). Still, galunisertib clearly inhibited SMAD2 phosphorylation in the presence and absence of TGF-β1 in rat and human PCLS (Figure 5).

TGF-β1 did not impact SMAD1 phosphorylation in rPCLS, hPCLS, and chPCLS (Figure 5). Yet, galunisertib concentration-dependently activated SMAD1 phosphorylation in rPCLS (Supporting Information Figure S3), in disparity to hPCLS and chPCLS, in which galunisertib had no effect on SMAD1 activation (Figure 5B-C).

Effect of galunisertib on collagens and ECM

To further determine the effect of galunisertib on collagens and ECM in human PCLS, a LDA was performed. Galunisertib significantly inhibited the expression of almost all collagen subtypes (collagen I, III, IV, V, and VI), as well as numerous genes associated with collagen maturation and homeostasis. The expression levels of noncollagenous ECM components commonly found in fibrosis were also decreased (Table 1). These anti-fibrotic effects of galunisertib were observed in both hPCLS and chPCLS, although the impact was more profound in chPCLS. Noteworthy, in chPCLS, galunisertib increased the expression of matrix metalloproteinase 13 (*MMP13*), which is involved in ECM degradation (Table 1).

In addition, galunisertib significantly decreased the release of pro-collagen I C-peptide (PICP) by both hPCLS and chPCLS, indicating a reduction in collagen type I production (Figure 6).
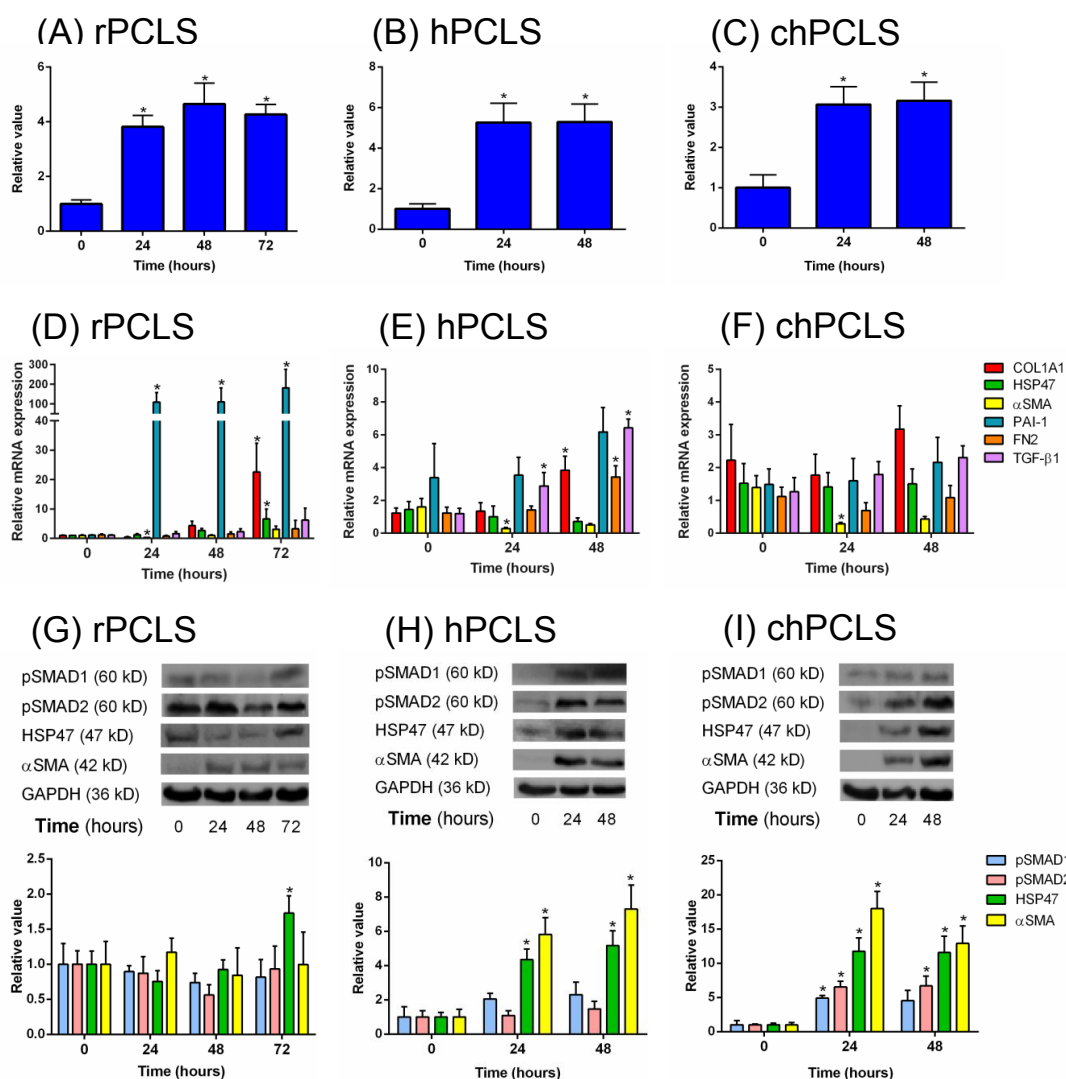
Chapter 4

Figure 1. General features of PCLS during incubation. (A-C) ATP level/protein, (D-F) gene, and (G-I) protein expression of r(rat)PCLS (A, D, G; n=5-6 per group), h(human)PCLS (B, E, H; n=4-8 per group), and ch(cirrhotic human)PCLS (C,F,I; n=3-6 per group), respectively. * $p<0.05$ compared to 0h. Representative sets of Western blots, and average protein expression (means ± SEM) of all experimental groups shown as bar graphs after normalization to GAPDH protein.
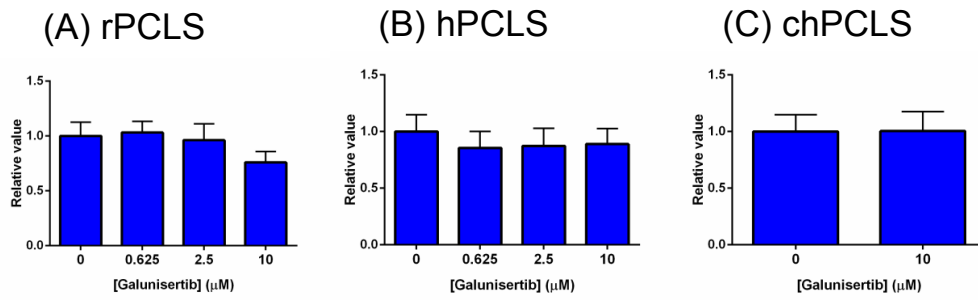
Figure 2. ATP level/protein of PCLS after treatment with galunisertib. (A; n=5) 72h in rPCLS, 48h in (B, n=8-9) hPCLS and (C, n=6) chPCLS.
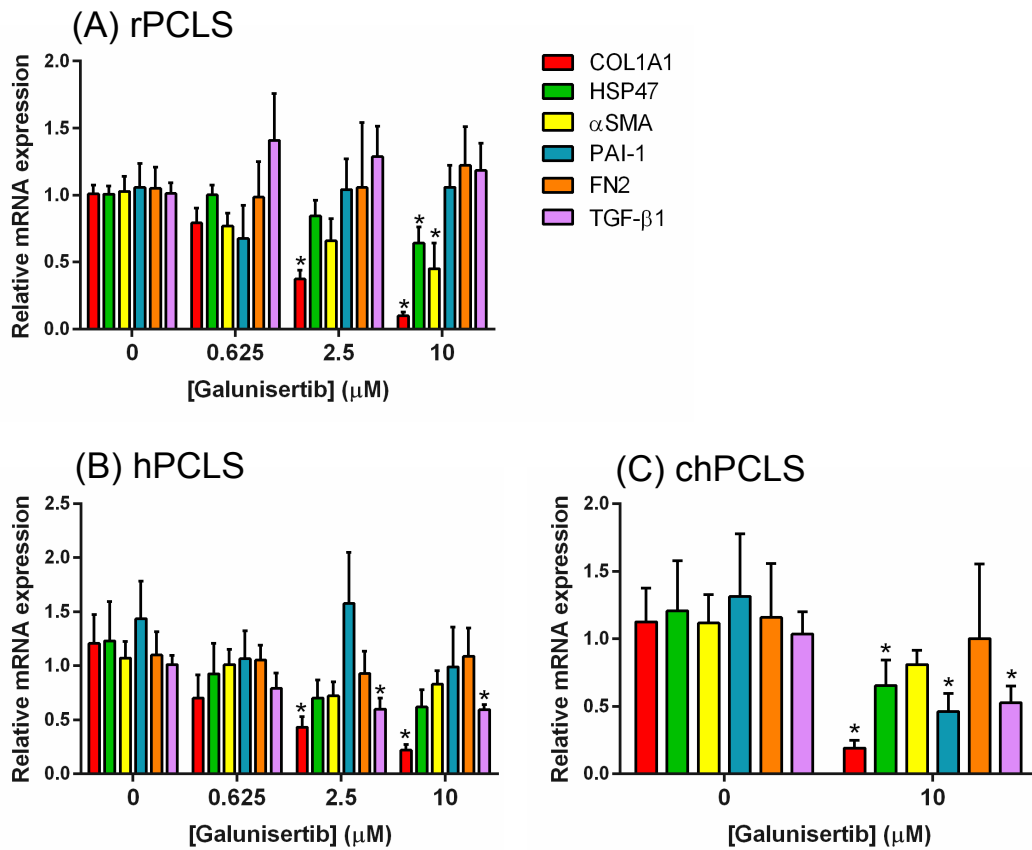
Figure 3. Fibrosis related gene expression after treatment with galunisertib. (A; n=5) for 72h in rPCLS, 48h in (B; n=5-8) hPCLS and (C; n=4-6) ChPCLS. * $p<0.05$ compared to control.

Chapter 4
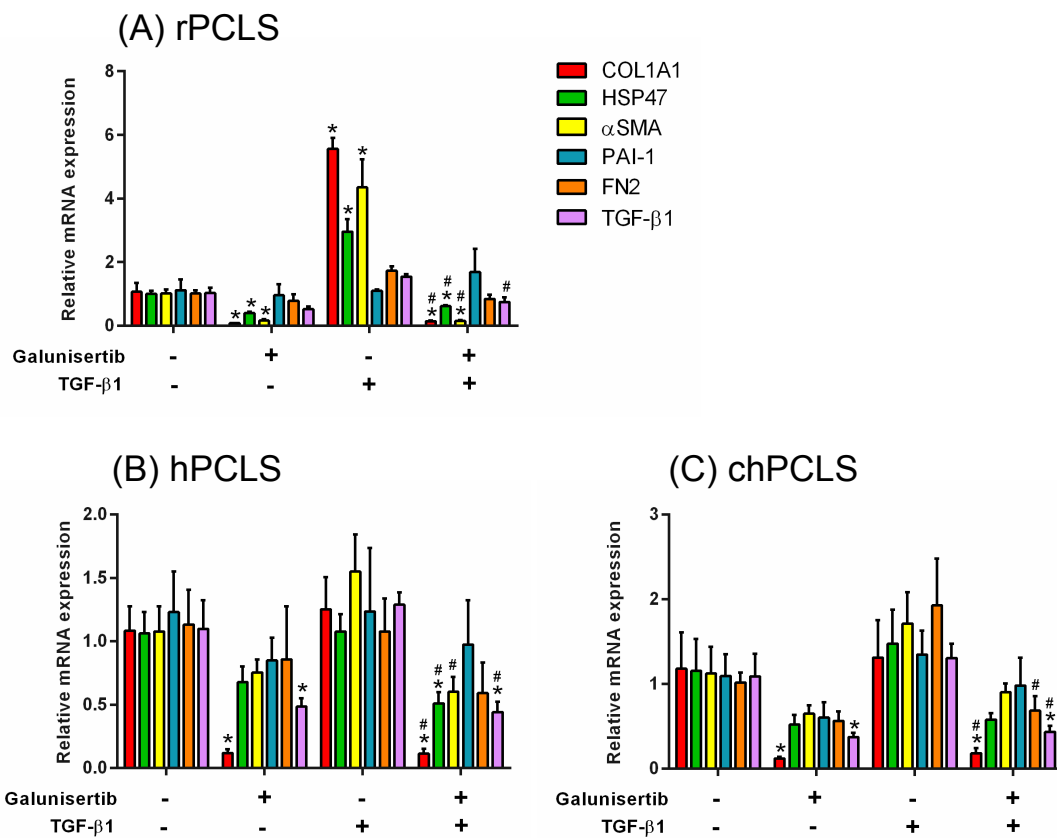
Figure 4. Fibrosis related gene expression after treatment with 10 µM galunisertib in the presence or absence of 1 ng/mL TGF-β1. (A; n=5) 72h in rPCLS, 48h in (B; n=5-6) hPCLS and (C; n=4) chPCLS. * and # $p<0.05$ compared to control and the TGF-β1-treated group, respectively.
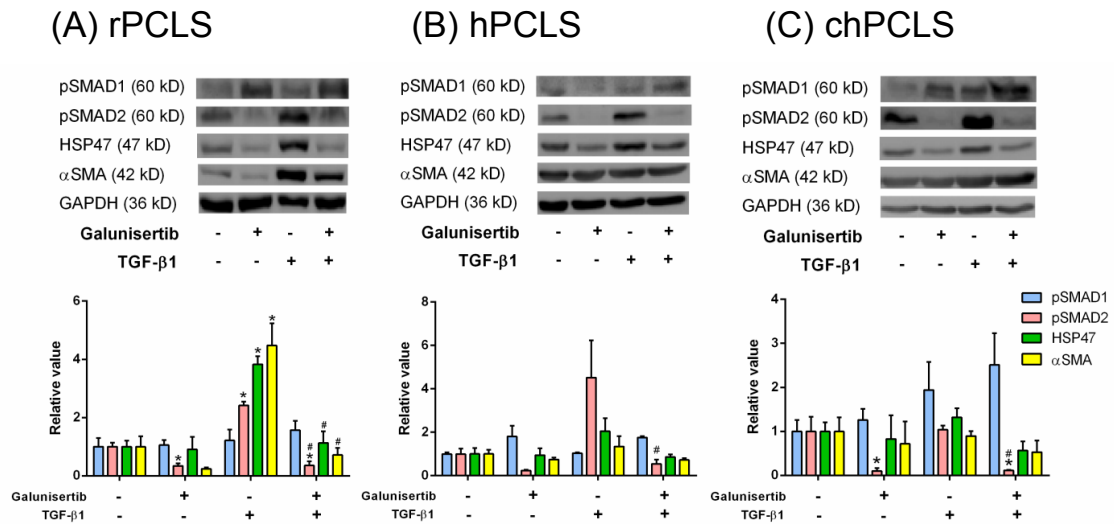
Figure 5. Phosphorylated SMADs and fibrogenic protein expression after treatment with 10 µM galunisertib in the presence or absence of 1 ng/mL TGF-β1. (A; n=6) 72h in rPCLS, 48h in (B; n=4) hPCLS and (C; n=4) chPCLS. * and # $p<0.05$ compared to control and the TGF-β1- treated group, respectively. Representative sets of Western blots, and average protein expression (means $\pm$ SEM) of all experimental groups shown as bar graphs after normalization to GAPDH protein.


Figure 6. Pro-collagen I C-peptide (PICP) released after treatment with galunisertib for 24h. (A; n=5) hPCLS and (B; n=3) chPCLS. * $p<0.05$ compared to control. Representative sets of Western blots, and average protein expression (means $\pm$ SEM) of all experimental groups shown as bar graphs.

75

Table 1
Expression of transcriptions related to different collagens, collagen maturation, noncollagenous ECM components, ECM remodeling, and select ECM receptors, by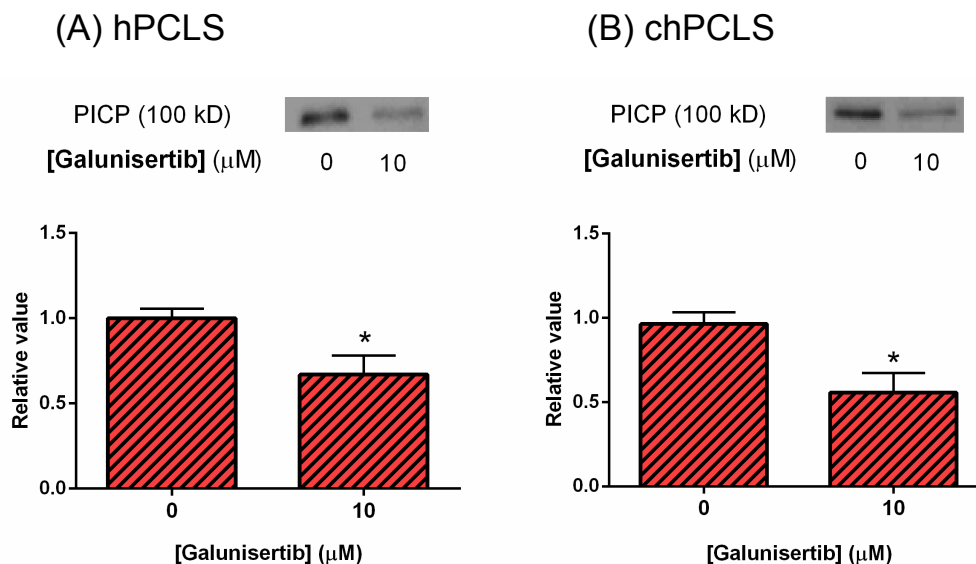 hPCLS and chPCLS after treatment with 10 μM galunisertib for 48h. Low Density Array (LDA), results are expressed as average fold induction ± SEM relative to GAPDH (n = 4).

Gene	hPCLS	chPCLS
Type of collagen		
COL1A1	↓ 0.13 ± 0.03*	↓ 0.13 ± 0.02*
COL1A2	↓ 0.40 ± 0.12*	↓ 0.26 ± 0.09*
COL3A1	↓ 0.46 ± 0.01*	↓ 0.33 ± 0.06*
COL4A1	↓ 0.31 ± 0.04*	↓ 0.28 ± 0.03*
COL5A1	↓ 0.37 ± 0.10*	↓ 0.20 ± 0.03*
COL6A1	↓ 0.67 ± 0.07*	↓ 0.63 ± 0.14
Collagen maturation		
PLOD1	↓ 0.54 ± 0.07*	↓ 0.75 ± 0.15
PLOD2	↓ 0.54 ± 0.22	↓ 0.49 ± 0.15
PLOD3	↓ 0.87 ± 0.17	↑ 1.12 ± 0.31
P4HA1	↑ 1.16 ± 0.26	↔ 0.95 ± 0.43
P4HA2	↔ 1.02 ± 0.37	↑ 1.45 ± 0.18
P4HA3	↓ 0.47 ± 0.13	↓ 0.22 ± 0.04*
P4HB	↓ 0.78 ± 0.08	↑ 1.17 ± 0.34
LEPRE1	↓ 0.75 ± 0.09	↓ 0.55 ± 0.12
LEPREL1	↓ 0.71 ± 0.13	↓ 0.51 ± 0.10*
LEPREL2	↓ 0.60 ± 0.15	↓ 0.82 ± 0.32
LOX	↔ 0.91 ± 0.58	↓ 0.51 ± 0.15
LOXL1	↓ 0.42 ± 0.13*	↓ 0.62 ± 0.19
LOXL2	↓ 0.49 ± 0.06*	↓ 0.34 ± 0.05*
LOXL3	↓ 0.81 ± 0.32	↓ 0.55 ± 0.16
LOXL4	↓ 0.40 ± 0.16	↓ 0.31 ± 0.09*
SERPINH	↓ 0.59 ± 0.12	↓ 0.43 ± 0.04*
ADAMTS2	↓ 0.70 ± 0.14	↓ 0.47 ± 0.16
ADAMTS3	↑ 1.97 ± 1.44	↓ 0.42 ± 0.09*
ADAMTS14	No expression	↓ 0.43 ± 0.17

Table 1 (continued)		
Collagen maturation		
BMP1	↓ 0.71 ± 0.07*	↓ 0.40 ± 0.07*
PCOLCE	↓ 0.75 ± 0.06*	↓ 0.30 ± 0.04*
PCOLCE2	↓ 0.83 ± 0.15	↓ 0.84 ± 0.44
FKBP10	↓ 0.47 ± 0.04*	↓ 0.38 ± 0.05*
SLC39A13	↔ 0.91 ± 0.08	↓ 0.79 ± 0.10
COLGALT1	↓ 0.78 ± 0.12	↓ 0.67 ± 0.14
Extracellular matrix component		
Fibronectin 1	↓ 0.13 ± 0.03*	↓ 0.13 ± 0.02*
Elastin	↓ 0.40 ± 0.12*	↓ 0.26 ± 0.09*
Decorin	↓ 0.46 ± 0.01*	↓ 0.33 ± 0.06*
Biglycan	↓ 0.31 ± 0.04*	↓ 0.28 ± 0.03*
Fibromodulin	↓ 0.37 ± 0.10*	↓ 0.20 ± 0.03*
Extracellular matrix remodelling		
MMP1	↑ 1.31 ± 0.44	↑ 1.95 ± 0.72
MMP13	No expression	↑ 6.37 ± 1.47*
MMP14	↓ 0.42 ± 0.02*	↓ 0.38 ± 0.05*
TIMP1	↓ 0.47 ± 0.03*	↓ 0.40 ± 0.10*
CTSK	↓ 0.70 ± 0.10	↓ 0.62 ± 0.15
Extracellular matrix protein receptor		
DDR1	↓ 0.65 ± 0.05*	↓ 0.55 ± 0.07*
DDR2	↔ 1.00 ± 0.21	↓ 0.42 ± 0.07*
MRC2	↓ 0.24 ± 0.07*	↓ 0.15 ± 0.02*

↓ indicates downregulation (fold induction <0.9).

↑ indicates upregulation (fold induction >0.9).

↔ indicates no difference (0.9≤ fold induction ≤1.1).

* indicates $p < 0.05$ compared to control.

Chapter 4

Discussion

Precision-cut liver slices (PCLS) are an effective *ex-vivo* model to study the potency and mechanism of action of putative anti-fibrotic compounds [22, 23]. As shown here, PCLS prepared from human and rat tissues are viable up to 48h and 72h, respectively. Furthermore, key fibrotic genes and proteins are spontaneously upregulated during culture. Therefore, the potency of anti-fibrotic compounds can be explored on both transcriptional and translational level. In addition, PCLS represent a model for the early-onset and end-stage of fibrosis, since they can be prepared from both healthy and diseased human livers. Results obtained with human PCLS would reasonably to be interpreted without concerns regarding species differences, a major caveat of the usual animal studies [22, 26].

Toxicity of galunisertib

Systemic inhibition of TGF-β signaling *in vivo* might interfere with various beneficial biological processes, which is an important concern for drug development. A severe adverse effect in animals treated with small molecule ALK5 inhibitors was hemorrhagic, degenerative, and inflammatory lesions in heart valve [27]. Nevertheless, based on impressive toxicity profiles in animal [17] and pharmacokinetic/pharmacodynamic relationship study [28], galunisertib was selected for clinical investigation.

A human pharmacokinetic study showed that, at steady state on day 14, the average maximum plasma concentration of galunisertib following 300 mg/day was 990 ng/mL or 2.68 μM [18]. This therapeutic dosage was deemed safe and is currently used in several clinical studies for the treatment of cancers. To date, these studies are ongoing without premature termination due to galunisertib-related toxicities [19, 20]. And also in our study, galunisertib appeared to be non-toxic to the liver as shown by stable ATP levels during experiments. Although the *ex vivo* concentrations cannot be compared to physiologic portal drug concentrations, the effective concentrations of galunisertib used in our study seem to be in line with the actual therapeutic concentrations attainable in patients.

Galunisertib mode of action in fibrosis

Our results demonstrated that galunisertib significantly inhibited TGF-β1 gene expression in the absence and especially in the presence of exogenous TGF-β1 in both hPCLS and chPCLS. In rat PCLS, the inhibitory effect was solely observed in the presence of TGF-β1. Due to the important role of TGF-β1 in fibrosis development and progression [9-12], our findings suggested that galunisertib which pharmacologically inhibits the actions of TGF-β1 should possess the potency for the treatment of liver fibrosis.

Galunisertib acts via inhibition of TGF-β receptor type I kinase activation. Therefore, the phosphorylation status of downstream signaling proteins, mainly SMAD1 and SMAD2, was used in our study to indicate the activation state of the TGF-β receptor. Galunisertib inhibited SMAD2 phosphorylation in rat and human PCLS, and these results are in line with previous studies targeting cancer cells [29, 30]. The important role of TGF-β1-meditated ALK5/SMAD2

phosphorylation in liver fibrosis and HSCs activation has been acknowledged by others [11, 12]. Thus, as observed in our study, the decrease in SMAD2 phosphorylation further underlines the anti-fibrotic potency of galunisertib. In contrast, after the treatment with galunisertib, SMAD1 phosphorylation was not inhibited in human PCLS; while significant upregulation of phosphorylated SMAD1 was observed in rat PCLS. Even though the role of TGF-β1-meditated ALK1/SMAD1 activation in liver fibrosis is poorly understood [15], the upregulation of SMAD1 phosphorylation in rats, but not in human, may be a compensatory pathway for the inhibition of ALK5/SMAD2. Nevertheless, the activation of ALK1/SMAD1 seems to be less significant for fibrogenesis compared to the net decrease of the fibrosis markers.

As galunisertib clearly showed anti-fibrotic efficacy in presence of exogenous TGF-β1 in rPCLS, interestingly, the anti-fibrotic potency of galunisertib was still displayed in human PCLS although the exogenous TGF-β1 could not further stimulate the expression levels of fibrosis related markers. In fact, it was anticipated because of previous studies that a further increase of the fibrosis related markers would not be observed in human PCLS in the presence of TGF-β1 [22]. Nevertheless, in our study, we aimed to show that galunisertib might exhibit anti-fibrotic potency via the inhibition of profibrotic spontaneous SMAD2 expression regardless of augmentative stimuli. On the other hand, galunisertib may possibly possess other mechanisms, irrespective of TGF-β1-related actions.

Effect of galunisertib on fibrosis markers

α-SMA is a well-known marker of activated HSCs. A previous study showed that the transcription level of α-SMA did not change during incubation in human PCLS [22]. Here, we show for the first time that, in contrast, α-SMA protein levels are increased during culture of PCLS. This controversy needs to be further investigated. Nevertheless, post-transcriptionally regulation of α-SMA in activated HSCs of human PCLS as observed in Dupuytren's nodular cells might be possible [31]. Interestingly, TGF-β1 did not further increase gene and protein expression of α-SMA in human PCLS, nor was the expression affected by galunisertib. On the other hand, in rat PCLS, α-Sma gene and protein expression were increased by TGF-β1 treatment, and galunisertib reduced the expression both in the absence and presence of TGF-β1. This discrepancy might indicate that the activation status of HSCs differs in human and rat PCLS at the start of experiments. This difference might arise due to partial activation of HSCs before or during surgery by stress and injury [32]. Importantly, this finding highlights the notion that observations in animal models may not be readily translatable to the human liver.

Our results further demonstrated that the expression of HSP47, a chaperone protein involved in intracellular collagen maturation [33, 34], was also affected by galunisertib. In rat PCLS, galunisertib clearly reduced both the gene and protein levels of HSP47, while only its gene expression was lowered in human PCLS. This discrepancy might again be caused by species differences, but also by a variant exposure to perioperative stress, injury, or constitutive expression, of the human samples [35]. It is also possible that longer incubation times are needed to see an impact of galunisertib on HSP47 protein levels in human PCLS.

Most importantly, the anti-fibrotic efficacy of galunisertib was clearly illustrated by the reduced collagen type I production in human hPCLS and chPCLS both on a transcriptional and translational level. Our results indicated that secretion of PICP, a by-product of collagen type I production, could be used as a marker of collagen production and fibrosis [35]. Although there are many types of collagen present in fibrotic lesions, collagen type I is the main ECM protein produced in liver fibrosis [36, 37].

We demonstrated that galunisertib not only downregulated collagen type I, but also collagen type III, IV, V, and VI. In addition, the expression of genes that encode enzymes associated with collagen maturation and fibril formation such as *LOXL2, FKBP10, BMP1*, and *PCOLCE*, was inhibited by galunisertib. These results suggest a unique effect of galunisertib on production, maturation, and formation of collagen fibrils. Moreover, galunisertib decreased the expression of fibronectin, which is recognized as an important ECM protein involved in liver fibrosis [38] as well as the levels of noncollagenous ECM proteins, *i.e.* elastin, decorin, biglycan, and fibromodulin. In addition, collagen and fibronectin receptors, *DDR1* and *MRC2*, were also decreased by galunisertib. These results highlight the uniquely broad effect of galunisertib on ECM formation.

The imbalance between ECM production and degradation is an important determinant in liver fibrosis progression [6]. Following treatment with galunisertib, a marked increase in the expression of matrix metalloproteinase-13 (*MMP13*), an enzyme that promotes collagen cleavage [39], was observed in chPCLS. Thus, galunisertib might also accelerate the degradation of ECM components in an ECM-rich environment as found in cirrhotic livers, which can be beneficial as well as detrimental. On the other hand, proteins that are normally increased during liver fibrosis, *i.e.* tissue inhibitor of metalloproteinases-1 (*TIMP1*) and *MMP14* [40, 41], were decreased by the action of galunisertib, supporting the beneficial property of this compound in the resolution of excessive ECM.

Conclusion

As illustrated in our human *ex vivo* study, galunisertib is a promising drug to be further investigated for the treatment of human liver fibrosis. Although, species-specific biological activity of compounds is widespread and a major hurdle in the development of effective therapeutics [22, 42], encouragingly, galunisertib exhibited its anti-fibrotic potency not only in rodent but also in humans PCLS. The inhibition of SMAD2 phosphorylation is probably the main mechanism underlying the anti-fibrotic effect of galunisertib. Moreover, the unique anti-fibrotic efficacy of galunisertib seems to be related to the production, maturation, formation, and degradation, of ECM.

Conflict of interest

No conflict of interest

Financial support

Acknowledgements

Chapter 4

Materials and methods

Human livers
Early-onset fibrosis was studied in PCLS prepared from surgical excess material of donor livers which were regarded as clinically healthy (hPCLS). End-stage fibrosis was studied in PCLS prepared from explanted cirrhotic livers of clinically diagnosed end-stage liver disease patients undergoing liver transplantation (chPCLS). The experimental protocols were approved by the Medical Ethical Committee of the University Medical Center Groningen.

Animal livers
Rat precision-cut liver slices (rPCLS) were prepared from adult male, 12-16 weeks old, Wistar rats, purchased from Charles River (Sulzfeld, Germany). The experiments were approved by the Animal Ethical Committee of the University of Groningen.

Precision-cut liver slices (PCLS)
PCLS were made as previously described [23]. The slices, with an estimated thickness of 250-300 μm, were exposed to galunisertib (Selleckchem, Munich, Germany) or solvent control (dimethyl sulfoxide; final concentration <0.4%) for 48h (human) and 72h (rat). The selected incubation periods correspond to the timeframe in which slices remain viable during culture [22]. Galunisertib was first tested at 0.625, 2.5, and 10 μM in rPCLS and hPCLS to identify the most effective concentration. Preliminary results indicated that 10 μM of galunisertib elicited a maximal effect whilst not influencing slice viability. Therefore, 10 μM, was used in subsequent experiments including chPCLS. For testing the potency of galunisertib in TGF-β1-induced fibrosis, the human recombinant TGF-β1 (Roche Diagnostics, Mannheim, Germany) was added in culture medium, containing 1 μg/mL bovine serum albumin, to yield 1 ng/mL TGF-β1. Every 24h, PCLS were transferred into new plates containing fresh culture medium.

ATP determination
Viability of PCLS was evaluated by assessing ATP content [24] using a bioluminescence kit (Roche Diagnostics). ATP values were corrected for the total protein content, estimated by the Lowry assay (Bio-Rad DC Protein Assay, Hercules, US), of each PCLS. Values for the treated groups are expressed as relative value as compared to the control group.

Quantitative real-time PCR and Low-Density Array (LDA)
Gene expression of multiple fibrosis related markers was assessed by quantitative real-time PCR and Low-Density Array (LDA). Total RNA was isolated from pooled snap-frozen PCLS (rPCLS and hPCLS: 3; chPCLS: 6) using the RNeasy Mini Kit (Qiagen, Venlo, the Netherlands). Reverse transcription was performed with 1 μg total RNA using the Reverse Transcription System (Promega, Leiden, the Netherlands) at 25 °C for 10 minutes, 45 °C for 60 minutes, and 95 °C for 5 minutes.

Gene expression was determined using specific primers (Supporting Information Table S1) and the SensiMix[TM] SYBR Hi-ROX kit (Bioline, Luckenwalde, Germany) on a 7900HT qPCR

system (Applied Biosystems) with a cycle at 95 ˚C for 10 minutes followed by 45 cycles of 95 ˚C for 15 seconds and 60 ˚C for 25 seconds. Expression levels were corrected using GAPDH as reference gene (ΔCt) and compared with the control group ($\Delta\Delta$Ct). Results are displayed as fold induction ($2^{-\Delta\Delta Ct}$).

LDA or Custom-made Taqman Array Microfluidic Cards (Applied Biosystems) with preloaded primers in 384-wells plates were used to elucidate the effects of galunisertib on 40 genes-related to fibrosis [25] (Supporting Information Table S2). 10 ng/µL cDNA was mixed with 2X Taqman PCR mastermix (Applied Biosystems). Thermal cycling and fluorescence detection were performed on a ViiA^{TM} 7 Real-Time PCR system (Applied Biosystems) with a cycle of 50 ˚C for 2 minutes and 95 ˚C for 10 minutes followed by 40 cycles of 90 ˚C for 15 seconds and 60 ˚C for 1 minute. Expression levels were corrected using GAPDH as reference gene (ΔCt) and compared with the control group ($\Delta\Delta$Ct). Results are displayed as fold induction ($2^{-\Delta\Delta Ct}$).

Western blotting

TGF-β1 signaling proteins, *i.e.* phosphorylated SMAD1 and SMAD2, and protein expression of key fibrosis markers were quantified by Western blotting. Three PCLS were pooled, snap frozen, and lysed. Total protein (100 µg) of PCLS lysates was separated on a 10% sodium dodecyl sulfate polyacrylamide gel and transferred to a polyvinylidene fluoride membrane. Immunodetection was performed by incubating the membranes with specific antibodies (Supporting Information Table S3). Targeted proteins were visualized with VisiGlo^{TM} Prime HRP Chemiluminescent Substrate Kit (Amresco, Ohio, US). Equal protein loading was confirmed by using GAPDH as internal control protein. Signal intensity was measured using ImageJ software (US National Institutes of Health). The data are expressed as relative value compared to the intensity of the control group.

Western blotting of pro-collagen I C-peptide (PICP) was performed under non-reduced conditions by precipitation of culture medium using 90% methanol. The total precipitated protein was redissolved and separated on a 7.5% sodium dodecyl sulfate polyacrylamide gel.

Statistics

Three to five livers were individually used for each experiment, using triplicate slices from each liver. The results are expressed as means ± SEM and compared to the control group using either Student's T-test or ANOVA followed by either Dunnett's or Tukey's post hoc analysis. A *p*-value less than 0.05 was considered significant. Statistical differences were determined on relative value of ATP, ΔCt for mRNA expression, and relative signal intensity of the proteins.

Supporting information

Table S1
Primers used in quantitative real-time PCR

Gene	Primer sequence	Human	Rat
α-SMA	Forward	AGGGGGTGATGGTGGGAA	AGCTCTGGTGTGTGACAATGG
	Reverse	ATGATGCCATGTTCTATCGG	GGAGCATCATCACCAGCAAAG
FN2	Forward	AGGCTTGAACCAACCTACGGATGA	TCTTCTGATGTCACCGCCAACTCA
	Reverse	GCCTAAGCACTGGCACAACAGTTT	TGATAGAATTCCTTGAGGGCGGCA
GAPDH	Forward	ACCAGGGCTGCTTTTAACTCT	GAACATCATCCCTGCATCCA
	Reverse	GGTGCCATGGAATTTGCC	CCAGTGAGCTTCCCGTTCA
HSP47	Forward	GCCCACCGTGGTGCCGCA	AGACGAGTTGTAGAGTCCAAGAGT
	Reverse	GCCAGGGCCGCCTCCAGGAG	ACCCATGTGTCTCAGGAACCT
COL1A1	Forward	CAATCACCTGCGTACAGAACGCC	CCCACCGGCCCTACTG
	Reverse	CGGCAGGGCTCGGGTTTC	GACCAGCTTCACCCTTAGCA
PAI-1	Forward	CACGAGTCTTTCAGACCAAG	AACCCAGGCCGACTTCA
	Reverse	AGGCAAATGTCTTCTCTTCC	CATGCGGGCTGAGACTAGAAT
TGF-β1	Forward	GCAGCACGTGGAGCTGTA	CCTGGAAAGGGCTCAACAC
	Reverse	CAGCCCGGTTGCTGAGGTA	CAGTTCTTCTCTGTGGAGCTGA

Table S2

Specifications of genes encoding collagens, collagen maturation, noncollagenous ECM components, ECM remodeling, and select ECM receptors, in Low-Density Array (LDA).

Gene and assay ID	Gene name
Type of collagen	
COL1A1-Hs00164004_m1	Collagen, Type I, Alpha 1
COL1A2-Hs00164099_m1	Collagen, Type II, Alpha 2
COL3A1-Hs00943809_m1	Collagen, Type III, Alpha 1
COL4A1-Hs00266237_m1	Collagen, Type IV, Alpha 1
COL5A1-Hs00609088_m1	Collagen, Type V, Alpha 1
COL6A1-Hs01095585_m1	Collagen, Type VI, Alpha 1
Collagen maturation	
PLOD1-Hs00609368_m1	Pro-collagen-Lysine, 2-Oxoglutarate 5-Dioxygenase 1
PLOD2-Hs00168688_m1	Pro-collagen-Lysine, 2-Oxoglutarate 5-Dioxygenase 2
PLOD3-Hs00153670_m1	Pro-collagen-Lysine, 2-Oxoglutarate 5-Dioxygenase 3
P4HA1-Hs00914594_m1	Prolyl 4-Hydroxylase, Alpha Polypeptide I
P4HA2-Hs00188349_m1	Prolyl 4-Hydroxylase, Alpha Polypeptide II
P4HA3-Hs00420085_m1	Prolyl 4-Hydroxylase, Alpha Polypeptide III
P4HB-Hs00168586_m1	Prolyl 4-hydroxylase subunit beta
LEPRE1-Hs00223565_m1	Leucine Proline-Enriched Proteoglycan (Leprecan) 1
LEPREL1-Hs00216998_m1	Leprecan-Like Protein 1
LEPREL2-Hs00204607_m1	Leprecan-Like Protein 2
LOX-Hs00942480_m1	Lysyl Oxidase
LOXL1-Hs00935937_m1	Lysyl Oxidase-Like Protein 1
LOXL2-Hs00158757_m1	Lysyl Oxidase-Like Protein 2
LOXL3-Hs01046945_m1	Lysyl Oxidase-Like Protein 3
LOXL4-Hs00260059_m1	Lysyl Oxidase-Like Protein 4
SERPINH1-Hs00241844_m1	Serpin Peptidase Inhibitor, Clade H; HSP47
ADAMTS2-Hs00247973_m1	ADAM Metallopeptidase with Thrombospondin Type 1 Motif, 2
ADAMTS3-Hs00610744_m1	ADAM Metallopeptidase with Thrombospondin Type 1 Motif, 3
ADAMTS14-Hs00365506_m1	ADAM Metallopeptidase with Thrombospondin Type 1 Motif, 14
BMP1-Hs00241807_m1	Bone Morphogenetic Protein 1
PCOLCE-Hs00170179_m1	Pro-collagen C-Endopeptidase Enhancer
PCOLCE2-Hs00203477_m1	Pro-collagen C-Endopeptidase Enhancer 2
FKBP10-Hs00222557_m1	FK506 Binding Protein 10
SLC39A13-Hs00378317_m1	Solute Carrier Family 39 (Zinc Transporter), Member 13
COLGALT1-Hs00430696_m1	Collagen Beta (1-O) Galactosyltransferase 1
Extracellular matrix component	
FN1-Hs00365052_m1	Fibronectin Type 1
ELN-Hs00355783_m1	Elastin
DCN-Hs00370385_m1	Decorin
BGN-Hs00959143_m1	Biglycan
FMOD-Hs00157619_m1	Fibromodulin
Extracellular matrix remodeling	
MMP1-Hs00899658_m1	Matrix Metalloproteinase 1
MMP13-Hs00233992_m1	Matrix Metalloproteinase 13
MMP14-Hs00237119_m1	Matrix Metalloproteinase 14
TIMP1-Hs99999139_m1	Tissue Inhibitor of Metalloproteinases 1
CTSK-Hs00166156_m1	Cathepsin K
Extracellular matrix protein receptor	

Chapter 4

DDR1-Hs00233612_m1	Discoidin Domain Receptor Tyrosine Kinase 1
DDR2-Hs00178815_m1	Discoidin Domain Receptor Tyrosine Kinase 2
MRC2-Hs00195862_m1	Mannose Receptor, C Type 2
Housekeeping protein	
GAPDH-Hs99999905_m1	Glyceraldehyde-3-Phosphate Dehydrogenase
B2M-Hs00187842_m1	Beta-2-Microglobulin
YWHAZ-Hs03044281_g1	Tyrosine 3-Monooxygenase/Tryptophan 5-Monooxygenase Activation Protein, Zeta
ACTB-Hs01060665_g1	Actin, Beta

Table S3

Buffer and antibodies used in Western blotting

Buffer ingredient

Lysis buffer: 30 mM Tris-HCl pH 7.4; 150 mM NaCl; 1 µM EDTA; 5.4 mg/mL Triton X-100; 1% SDS; 15 mM sodium orthovanadate; 15 mM sodium fluoride; a tablet/50 ml of PhosSTOP™ (Roche Diagnostics, Mannheim, Germany).

SDS sample buffer: 50 mM Tris-HCl pH 6.8; 2% SDS; 10% glycerol; 1% beta-mercaptoethanol; 0.0125% bromophenol blue.

Blocking buffer: 50 mM Tris-HCL pH 7.6; 150 nM NaCl, 5% non-fat dry milk (Blocking Grade Powder, Biorad); 0.1% Tween-20.

| Antibody and dilution	Manufacturer
Anti-α-smooth muscle actin (α-SMA), 1:5000	Sigma, Saint Louis, US
Anti-glyceraldehyde 3-phosphate dehydrogenase (GAPDH), 1:5000	Sigma, Saint Louis, US
Anti-heat shock protein 47 (HSP47), 1:2000	Abcam, Cambridge, UK
Anti-pro-collagen I C-peptide antibody (PICP), 1: 1000	Thermo Fisher, Rockford, US
Anti-phospho-SMAD1/5 (Ser463/465), 1:1000	Cell Signaling, Danvers, US
Anti-phospho-SMAD2 (Ser465/467), 1:1000	Cell Signaling, Danvers, US
Polyclonal goat anti-rabbit immunoglobulins/HRP, 1:2000	Dako, Glostrup, Denmark
Polyclonal rabbit anti-mouse immunoglobulins/HRP, 1: 2000	Dako, Glostrup, Denmark

Chapter 4

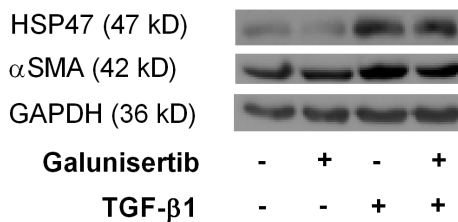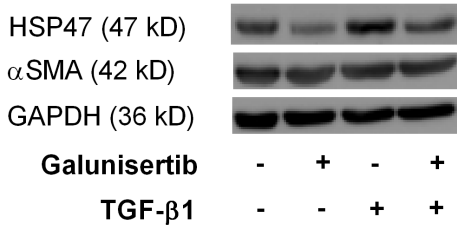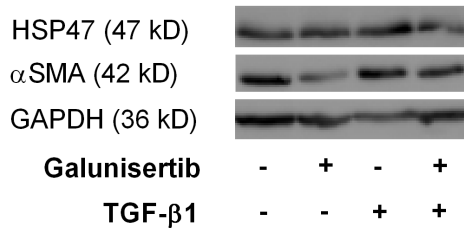(A) rPCLS/hPCLS/chPCLS   (B) hPCLS/chPCLS
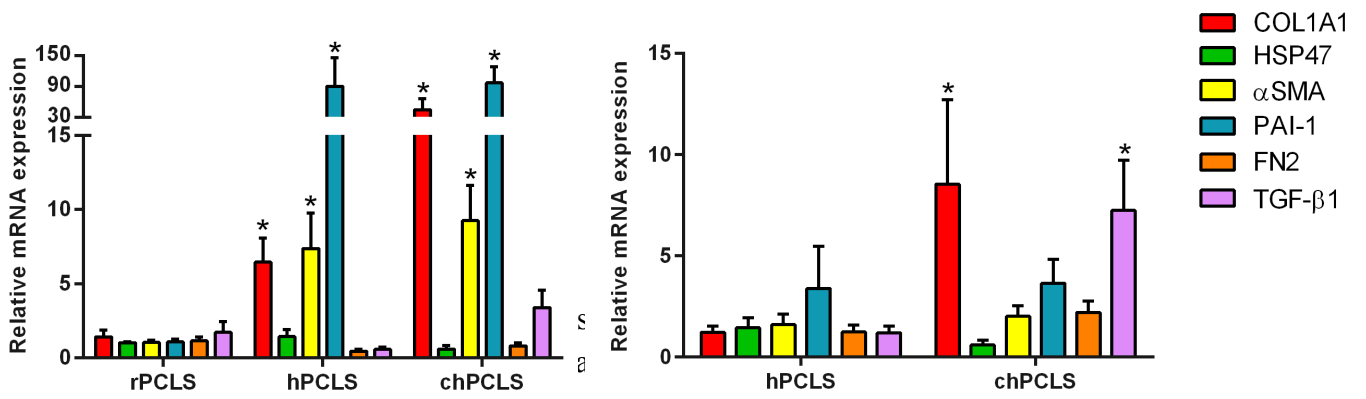
Figure S1

Comparison of fibrosis related gene expression at 0h. (A; n=4-8) among rPCLS, hPCLS and chPCLS, and (B; n=4-8) between hPCLS and chPCLS. * $p<0.05$ compared to (A) rPCLS or (B) hPCLS.
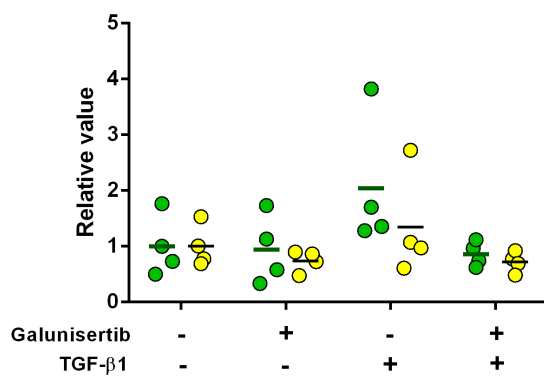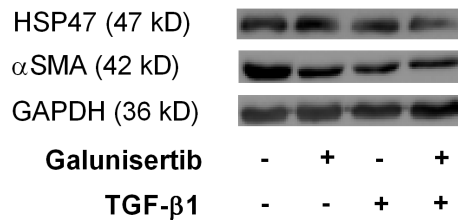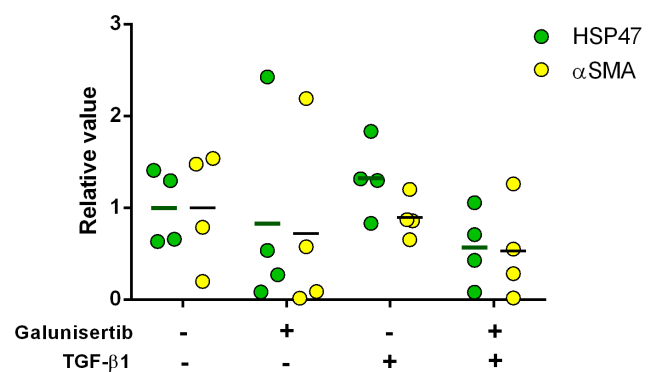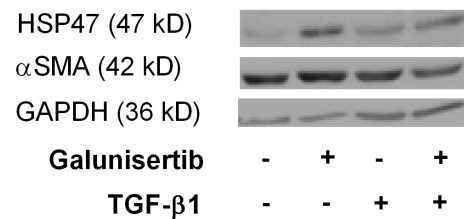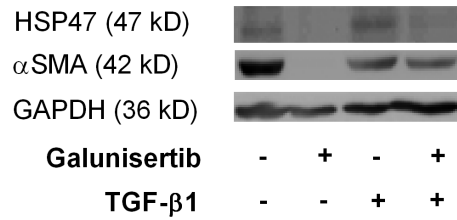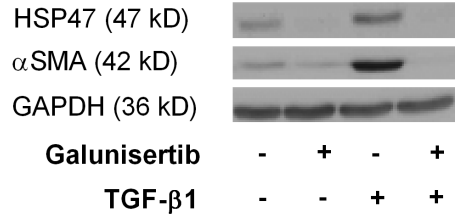
(A) hPCLS (B) chPCLS
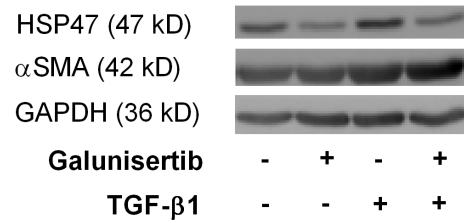
Figure S2

Scatter plots of HSP47 and α-SMA protein expression after treatment with 10 μM galunisertib in the presence or absence of 1 ng/mL TGF-β1 for 48h. (A; n=4) hPCLS and (B; n=4) chPCLS. Exemplary Western blots, avera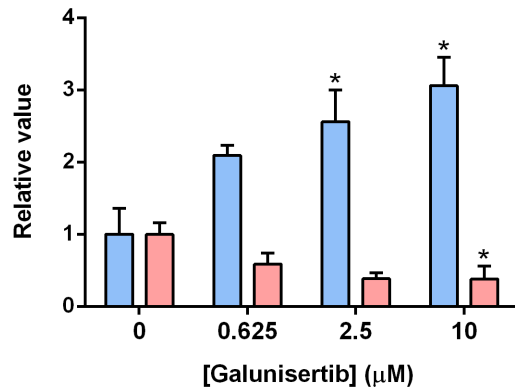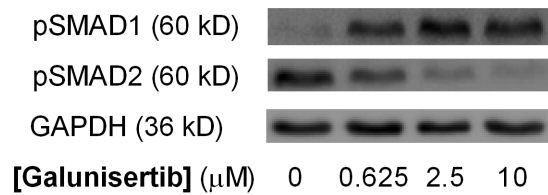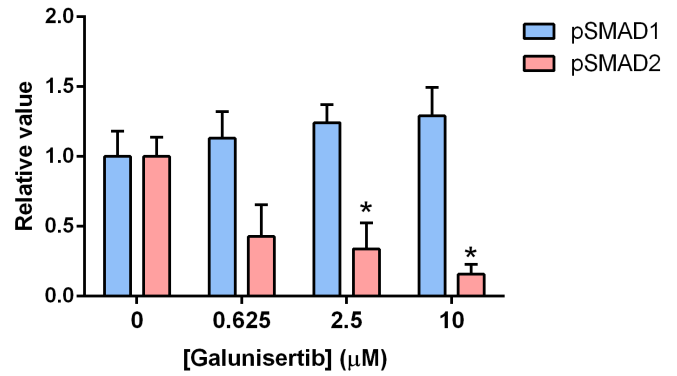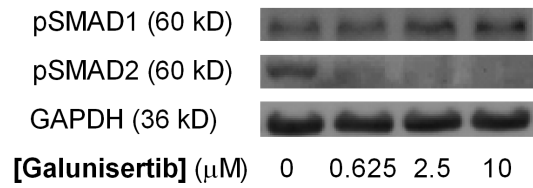ges of all experimental groups and scatter plots indicating individual band intensities after normalization to GAPDH protein.

(A) rPCLS

pSMAD1 (60 kD)

pSMAD2 (60 kD)

GAPDH (36 kD)

[Galunisertib] (μM)   0   0.625 2.5   10

(B) hPCLS

pSMAD1 (60 kD)

pSMAD2 (60 kD)

GAPDH (36 kD)

[Galunisertib] (μM)   0   0.625 2.5   10

Figure S3

Phosphorylated SMADs after treatment with 0.625, 2.5, and 10 μM galunisertib. (A; n=3) 72h in rPCLS and (B; n=3-4) 48h in hPCLS. * $p<0.05$ compared to control. Representative sets of Western blots, and average protein expression (means ± SEM) of all experimental groups shown as bar graphs after normalization to GAPDH protein.

References

1. Southan, C., et al., The IUPHAR/BPS Guide to PHARMACOLOGY in 2016: towards curated quantitative interactions between 1300 protein targets and 6000 ligands. Nucleic Acids Res, 2016. 44(D1): p. D1054-68.

2. Alexander, S.P., et al., The Concise Guide to PHARMACOLOGY 2015/16: Catalytic receptors. Br J Pharmacol, 2015. 172(24): p. 5979-6023.

3. Alexander, S.P., et al., The Concise Guide to PHARMACOLOGY 2015/16: Enzymes. Br J Pharmacol, 2015. 172(24): p. 6024-109.

4. Trautwein, C., et al., Hepatic fibrosis: Concept to treatment. J Hepatol, 2015. 62(1 Suppl): p. S15-24.

5. Torok, N.J., et al., Strategies and endpoints of anti-fibrotic drug trials: Summary and recommendations from the AASLD Emerging Trends Conference, Chicago, June 2014. Hepatology, 2015. 62(2): p. 627-34.

6. Schuppan, D. and N.H. Afdhal, Liver cirrhosis. The Lancet, 2008. 371(9615): p. 838-851.

7. Zarrinpar, A. and R.W. Busuttil, Liver transplantation: past, present and future. Nat Rev Gastroenterol Hepatol, 2013. 10(7): p. 434-40.

8. Giannelli, G., E. Villa, and M. Lahn, Transforming growth factor-beta as a therapeutic target in hepatocellular carcinoma. Cancer Res, 2014. 74(7): p. 1890-4.

9. Akhurst, R.J. and A. Hata, Targeting the TGFbeta signalling pathway in disease. Nat Rev Drug Discov, 2012. 11(10): p. 790-811.

10. Dooley, S. and P. ten Dijke, TGF-beta in progression of liver disease. Cell Tissue Res, 2012. 347(1): p. 245-56.

11. Dooley, S., et al., Modulation of transforming growth factor beta response and signaling during transdifferentiation of rat hepatic stellate cells to myofibroblasts. Hepatology, 2000. 31(5): p. 1094-106.

12. Hellerbrand, C., et al., The role of TGFbeta1 in initiating hepatic stellate cell activation in vivo. J Hepatol, 1999. 30(1): p. 77-87.

13. Yang, L., et al., Transforming growth factor-beta signaling in hepatocytes promotes hepatic fibrosis and carcinogenesis in mice with hepatocyte-specific deletion of TAK1. Gastroenterology, 2013. 144(5): p. 1042-1054 e4.

14. Schmierer, B. and C.S. Hill, TGFbeta-SMAD signal transduction: molecular specificity and functional flexibility. Nat Rev Mol Cell Biol, 2007. 8(12): p. 970-82.

15. Munoz-Felix, J.M., M. Gonzalez-Nunez, and J.M. Lopez-Novoa, ALK1-Smad1/5 signaling pathway in fibrosis development: friend or foe? Cytokine Growth Factor Rev, 2013. 24(6): p. 523-37.

16. Wiercinska, E., et al., Id1 is a critical mediator in TGF-beta-induced transdifferentiation of rat hepatic stellate cells. Hepatology, 2006. 43(5): p. 1032-41.

17. Herbertz, S., et al., Clinical development of galunisertib (LY2157299 monohydrate), a small molecule inhibitor of transforming growth factor-beta signaling pathway. Drug Des Devel Ther, 2015. 9: p. 4479-99.

18. Rodon, J., et al., Pharmacokinetic, pharmacodynamic and biomarker evaluation of transforming growth factor-beta receptor I kinase inhibitor, galunisertib, in phase 1 study in patients with advanced cancer. Invest New Drugs, 2015. 33(2): p. 357-70.

19. Eli-Lilly. A study of galunisertib (LY2157299) in combination with nivolumab in advanced refractory solid tumors and in recurrent or refractory NSCLC, hepatocellular carcinoma, or glioblastoma. 2015 November 16, 2016 [cited 2017 January 13]; Available from: https://clinicaltrials.gov/ct2/show/study/NCT02423343.

20. Eli-Lilly. A study of LY2157299 in participants with hepatocellular carcinoma. 2010 December 9, 2016 [cited 2017 January 13]; Available from: https://clinicaltrials.gov/ct2/show/NCT01246986.

21. Westra, I.M., et al., The effect of anti-fibrotic drugs in rat precision-cut fibrotic liver slices. PLoS One, 2014. 9(4): p. e95462.

22. Westra, I.M., et al., Human precision-cut liver slices as a model to test anti-fibrotic drugs in the early-onset of liver fibrosis. Toxicol In Vitro, 2016. 35: p. 77-85.

23. Olinga, P. and D. Schuppan, Precision-cut liver slices: a tool to model the liver ex vivo. J Hepatol, 2013. 58(6): p. 1252-3.

24. de Graaf, I.A., et al., Preparation and incubation of precision-cut liver and intestinal slices for application in drug metabolism and toxicity studies. Nat Protoc, 2010. 5(9): p. 1540-51.

25. Remst, D.F., et al., Gene expression analysis of murine and human osteoarthritis synovium reveals elevation of transforming growth factor beta-responsive genes in osteoarthritis-related fibrosis. Arthritis Rheumatol, 2014. 66(3): p. 647-56.

26. Stribos, E.G., et al., Precision-cut human kidney slices as a model to elucidate the process of renal fibrosis.

Transl Res, 2016. 170: p. 8-16 e1.

27.   de Gramont, A., S. Faivre, and E. Raymond, Novel TGF-beta inhibitors ready for prime time in onco-immunology. Oncoimmunology, 2017. 6(1): p. e1257453.

28.   Gueorguieva, I., et al., Defining a therapeutic window for the novel TGF-β inhibitor LY2157299 monohydrate based on a pharmacokinetic/pharmacodynamic model. British Journal of Clinical Pharmacology, 2014. 77(5): p. 796-807.

29.   Serova, M., et al., Effects of TGF-beta signalling inhibition with galunisertib (LY2157299) in hepatocellular carcinoma models and in ex vivo whole tumor tissue samples from patients. Oncotarget, 2015. 6(25): p. 21614-27.

30.   Maier, A., et al., Anti-tumor activity of the TGF-beta receptor kinase inhibitor galunisertib (LY2157299 monohydrate) in patient-derived tumor xenografts. Cell Oncol (Dordr), 2015. 38(2): p. 131-44.

31.   Verjee, L.S., et al., Post-transcriptional regulation of alpha-smooth muscle actin determines the contractile phenotype of Dupuytren's nodular cells. J Cell Physiol, 2010. 224(3): p. 681-90.

32.   Lau, D.T., et al., Intrahepatic gene expression profiles and alpha-smooth muscle actin patterns in hepatitis C virus induced fibrosis. Hepatology, 2005. 42(2): p. 273-81.

33.   Ishida, Y. and K. Nagata, Hsp47 as a collagen-specific molecular chaperone. Methods Enzymol, 2011. 499: p. 167-82.

34.   Mala, J.G. and C. Rose, Interactions of heat shock protein 47 with collagen and the stress response: an unconventional chaperone model? Life Sci, 2010. 87(19-22): p. 579-86.

35.   Brown, K.E., et al., Expression of HSP47, a collagen-specific chaperone, in normal and diseased human liver. Lab Invest, 2005. 85(6): p. 789-97.

36.   Yamamoto, M., et al., Distribution of collagen types I, III, and V in fibrotic and neoplastic human liver. Acta Pathol Jpn, 1984. 34(1): p. 77-86.

37.   Voss, B., et al., Distribution of collagen type I and type III and of two collagenous components of basement membranes in the human liver. Pathol Res Pract, 1980. 170(1-3): p. 50-60.

38.   Altrock, E., et al., Inhibition of fibronectin deposition improves experimental liver fibrosis. J Hepatol, 2015. 62(3): p. 625-33.

39.   Endo, H., et al., Matrix metalloproteinase-13 promotes recovery from experimental liver cirrhosis in rats. Pathobiology, 2011. 78(5): p. 239-52.

40.   Busk, T.M., et al., TIMP-1 in patients with cirrhosis: relation to liver dysfunction, portal hypertension, and hemodynamic changes. Scand J Gastroenterol, 2014. 49(9): p. 1103-10.

41.   Takahara, T., et al., Dual expression of matrix metalloproteinase-2 and membrane-type 1-matrix metalloproteinase in fibrotic human livers. Hepatology, 1997. 26(6): p. 1521-9.

42.   Iswandana, R., et al., Organ- and species-specific biological activity of rosmarinic acid. Toxicol In Vitro, 2016. 32: p. 261-8.